

## Mechanical properties of self-welded silicon nanobridges

Massood Tabib-Azar,<sup>a)</sup> Maissarath Nassirou, and Run Wang  
*Electrical Engineering and Computer Science Department, Case Western Reserve University, Cleveland, Ohio 44106*

S. Sharma, T. I. Kamins, M. Saif Islam, and R. Stanley Williams  
*Quantum Science Research, Hewlett-Packard Laboratories, Palo Alto, California 94304*

(Received 18 April 2005; accepted 15 July 2005; published online 6 September 2005)

Mechanical properties of self-welded [111] single-crystal silicon nanowire bridges grown between two silicon posts using metal-catalyzed chemical vapor deposition were determined using both dynamic and static measurements. The static tests were carried out using atomic force microscopy (AFM) to measure the nanowires' Young's modulus and the strength of the self-welded junctions. The AFM-measured Young's modulus ranged from 93 to 250 GPa (compared to 185 GPa for bulk silicon in the [111] direction) depending on the nanowire diameter, which ranged from 140 to 200 nm. The self-welded wire could withstand a maximum bending stress in the range of 210–830 MPa (larger than bulk silicon), which also depended on the nanowire diameter and loading conditions. The beam broke close to the loading point, rather than at the self-welded junction, indicating the excellent bond strength of the self-welded junction. The vibration spectra measured with a network analyzer and a dc magnetic field indicated a dynamic Young's modulus of 140 GPa, in good agreement (within the experimental error) with the static measurement results. © 2005 American Institute of Physics. [DOI: 10.1063/1.2042549]

Self-assembled silicon nanowires<sup>1,2</sup> may find interesting applications in gas and chemical sensors, electronics, and nanoelectromechanical systems with resonant frequencies in the gigahertz range suitable for clocks and nanobalance (similar to microbalance) sensing devices. The mechanical properties of millimeter-to-micrometer-scale Si-based structures have been extensively investigated,<sup>3,4</sup> and here we extend these studies to silicon nanowires grown between two silicon posts using metal-catalyzed chemical vapor deposition (MCCVD).

Most nanowires studied previously were manually assembled using micromanipulators or atomic force microscope (AFM) probes. The MCCVD-grown nanowires studied here were self-assembled and self-welded to two silicon posts as described in Refs. 1 and 5. Thus, the test results are much more reproducible than those for manually assembled wires. One primary objective of the present study was to understand how strongly these nanowires are welded to the silicon posts and which side (base or self-welded side) had a larger bond strength. We were also interested in measuring the nanowires' Young's modulus and its maximum bending stress. Although it is possible to excite and characterize the nanowires electrostatically, the magnetomotive technique<sup>2</sup> is better suited to nanoscale wires, and was used here for dynamic testing. For static load and bond-strength measurements, we used the AFM technique.

The nanobridge samples were prepared and grown at Quantum Science Research, Hewlett-Packard Laboratories. Electrically isolated electrodes were formed from the top Si (110) layer of a silicon-on-insulator structure.<sup>5</sup> Approximately 1 nm Au was deposited on the sides of the electrodes and annealed in a H<sub>2</sub> ambient at 670 °C. The Au was removed from the bottom oxide, and the structure was further

annealed and then exposed to a mixture of 15 sccm SiH<sub>4</sub>, 60 sccm HCl, and 30 sccm B<sub>2</sub>H<sub>6</sub> (100 ppm in H<sub>2</sub>) in a H<sub>2</sub> ambient at 680 °C for 30 min. The nanowire axial growth rate under these conditions is approximately 400 nm/min. Thus, the nanowires bridge across spaces between electrodes that are <12 μm. The silicon nanowires were single crystal with [111] growth axis. A scanning electron microscope (SEM) image of the region between the two sidewalls (Fig. 1) shows silicon nanowires that are either cantilevers or bridges. These two configurations allowed us to measure the effective Hooke's constant using the static AFM technique and to estimate the tension in the bridge configuration. In the dynamic tests, the bridge configuration was used.

For the resonance frequency measurements, the samples were mounted onto a chip carrier and contacted with aluminum wires using silver epoxy. The nanowire lengths were approximately 10 μm, and their diameters varied from 100 to 200 nm.

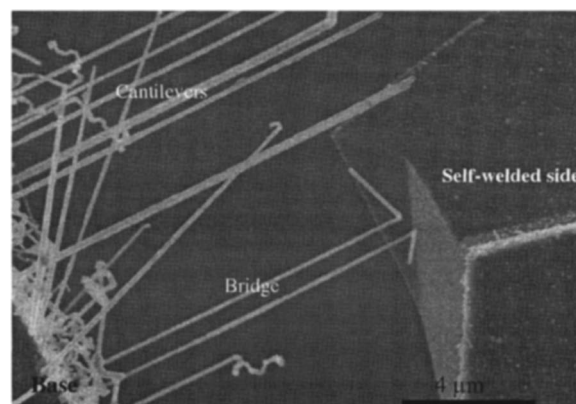


FIG. 1. SEM image of the region between two posts, showing both single-clamped (cantilever) and double-clamped (bridge) nanowire beam configurations.

<sup>a)</sup> Author to whom correspondence should be addressed; electronic mail: tabib-azar@case.edu

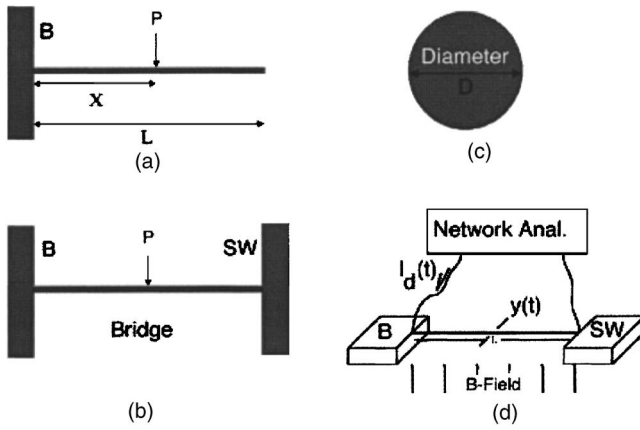


FIG. 2. Experimental configuration for measuring the mechanical properties of silicon nanowires. (a) Side view of the cantilever nanowire. (b) Side view of the bridge nanowire. The wires were grown from the base end (denoted by B) and are self-welded to the opposing post (denoted by SW). The force  $P$  in (a) and (b) is applied using an AFM. (c) Nanowire cross sections are typically circular with diameter  $D$ . (d) The setup used in magnetomotive dynamic measurement of nanowire beam (with length  $L$ ) resonance frequency.

Electromechanical characteristics were measured using the magnetomotive detection technique with static uniform magnetic fields. A double-clamped silicon nanowire with length  $L$ , and diameter  $D$ , has a fundamental resonance frequency

$$f_0 = 1.03 \sqrt{\frac{E D}{\rho L^2}}, \quad (1)$$

where  $E$  is Young's modulus and  $\rho$  is the density. A driving force is generated on the resonator by placing it in a uniform magnetic field  $B$  parallel to the resonator plane, and passing through the resonator a current  $I_D(t)$  perpendicular to the magnetic field as schematically shown in Fig. 2. A Lorentz force  $F_D(t) = LB I_D(t)$  is thereby developed through the motion of the resonator (initially generated by random fluctuation) in the applied magnetic field. The motion of the resonator through the magnetic field generates an electromotive force along the leads of the resonator,  $V_{EMF}(t) = \xi L B d y(t) / dt$ , where  $\xi$  is a constant of order unity that depends on the mode shape, and  $y(t)$  is the displacement of the midpoint of the resonator. A network analyzer was used to drive an alternating current through the beam and measure the response of the beam as shown in Fig. 3. In Eq. (1), we assume that the density of the silicon nanowires is similar to that of bulk Si  $\rho = 2330 \text{ kg/m}^3$ .

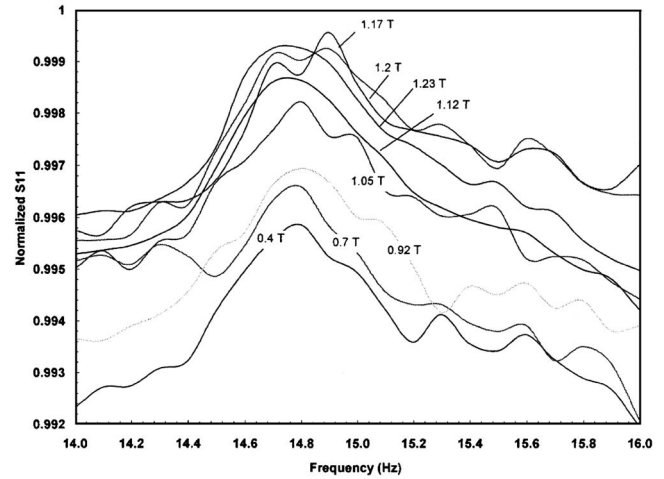


FIG. 3. Magnetomotive oscillation spectra of nanowires for different magnetic fields.

Mechanical testing was performed using an AFM (Nanoscope IV Multi-Mode, Digital Instruments). After obtaining an AFM image of the nanowires, we chose specific locations on the samples where bending tests were performed. The experimental arrangement for the bending test is illustrated in Figs. 2(a) and 2(b). After the AFM tip was in contact with the nanowire, a displacement in steps of 110 nm was applied to the tip, and the corresponding force was measured. The calculations of bending stresses and Young's modulus are explained below. For the circular cross section [Fig. 2(c)], the section modulus  $S$  and the bending stress  $\sigma$  are given by:

$$S = \pi D^3 / 32, \quad (2)$$

$$\sigma = -M / S, \quad (3)$$

respectively, where  $M$  is the maximum bending moment. Furthermore, from the measured deflection  $\delta$ , the Young's modulus  $E$ , is calculated.

$$\delta = P x^2 (3L - x) / 6EI, \text{ and} \quad (4)$$

$$E = m x^2 (3L - x) / 6I, \quad (5)$$

where  $P$  is the applied load,  $m$  is the gradient of the load-deflection curve, and  $I$  is the moment of inertia given by  $I = \pi d^4 / 64$  for a circular cross section. Three nanowires were tested: Sample I was a single-clamped cantilever while Samples II and III were double-clamped bridges. All nanowires were 10  $\mu\text{m}$  long.

The resonance frequency measurements [Fig. 3] show that the beams vibrate in their fundamental in-plane mode

TABLE I. Static and dynamic Young's modulus ( $E$ ) and maximum bending stress determined using AFM and magnetomotive force measurements.

	Diameter (nm)	Static $E$ (GPa)	Loading location <sup>a</sup> ( $\mu\text{m}$ )	Dynamic $E$ (GPa) ( $f_0 \sim 14.8 \text{ MHz}$ )	Bending stress (MPa)
Sample I (Cantilever)	140	93	3		852
Sample II (Bridge)	200	150	3.3		300
Sample III (Bridge)	200	250	5		560
Sample IV (Bridge)	150			140	

<sup>a</sup>The loading position was measured from the wire base side.

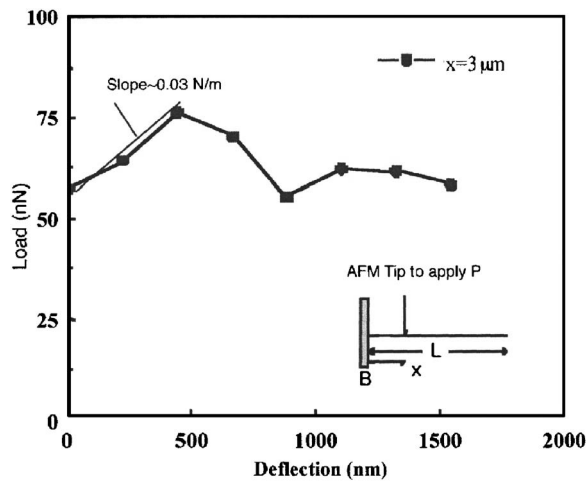


FIG. 4. Force vs displacement (load-deflection) behavior measured using AFM for a cantilever silicon nanowire (Sample I in Table I) at  $x=3 \mu\text{m}$  from the base end. Young's modulus is determined from the linear region below 500 nm deflection.

with a measured resonant frequency  $f_0=14.8 \text{ MHz}$  under magnetic fields varying from 0 T to 1.23 T. The corresponding Young's modulus depends largely on the nanowire diameter, and it is approximately 140 GPa in nanowires with a 150 nm diameter.

The static load-deflection curves for cantilever beams and bridges are shown in Figs. 4 and 5, respectively. When the load was applied close to the base end of the beam (Fig. 5,  $x=L/4$ ), the beam fractured close to the loading point. When the load was applied in the center of the beam, the

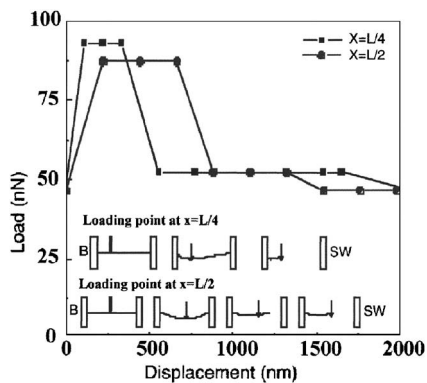


FIG. 5. Load-deflection curves obtained for nanowire bridge beams for Samples II ( $x=L/4$ ) and III ( $x=L/2$ ).

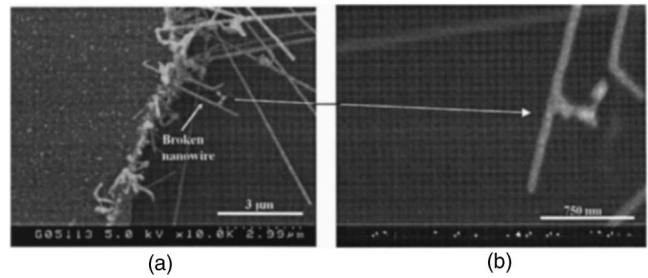


FIG. 6. (a) SEM image near base end of nanowires broken during mechanical testing. (b) A higher magnification view of the broken nanowire shown in (a).

fracture occurred in two steps. Initially, the beam seemed to fracture, but was still connected at both ends. With further loading, the fractured beam became disconnected in a region close to the loading point (Fig. 5,  $X=L/2$ ). These features on the load-deflection curves indicate that the nanowires are strongly attached to both the base end and the self-welded end.

Using Eqs. (2)–(5), both the Young's modulus and the bending stresses were calculated and are summarized in Table I. The SEM investigation of the nanowires after the bending tests (Fig. 6) shows that the nanowires do not fracture at the junctions between the nanowire and the vertical sidewalls. The calculated maximum bending stresses varied between 300 and 850 MPa, while Young's modulus was in the range of 93–250 GPa. Because the nanowires were not in plane, determining their diameters gave rise to an uncertainty of  $\pm 25 \text{ nm}$ . After taking measurement errors into account, we found a Young's modulus of  $210 \pm 40 \text{ GPa}$ . Within the experimental uncertainty, this value is comparable to the reported value of 185 GPa,<sup>2</sup> for the Young's modulus of bulk silicon in the [111] direction.<sup>2</sup>

The work at Hewlett-Packard was partially supported by the Defense Advanced Research Projects Agency. The work at Case was partially supported by a NSF NER grant (under Dr. Sankar Basu).

<sup>1</sup>M. Saif Islam, S. Sharma, T. I. Kamins, and R. Stanley Williams, *Nanotechnology* **15**, L5 (2004).

<sup>2</sup>A. N. Cleland and M. L. Roukes, *Sens. Actuators, A* **72**, 256 (1999).

<sup>3</sup>S. Sundararajan, B. Bhushan, T. Namazu, and Y. Isono, *Ultramicroscopy* **94**, 111 (2002).

<sup>4</sup>T. Namazu, Y. Isono, and T. Tanake, *J. Microelectromech. Syst.* **11**, 125 (2002).

<sup>5</sup>M. Saif Islam, S. Sharma, T. I. Kamins, and R. Stanley Williams, *Appl. Phys. A: Mater. Sci. Process.* **80**, 1133 (2005).